

1 **Supplementary Information**

2 **p140Cap inhibits β -Catenin in the breast cancer stem cell compartment instructing a protective**
3 **anti-tumor immune response**

4 Vincenzo Salemme^{1,2}, Mauro Vedelago¹, Alessandro Sarcinella¹, Federico Moietta¹, Alessio
5 Piccolantonio^{1,2}, Enrico Moiso¹, Giorgia Centonze^{1,2}, Marta Manco¹, Andrea Guala¹, Alessia
6 Lamolinara³, Costanza Angelini¹, Alessandro Morellato^{1,2}, Dora Natalini¹, Raffaele Calogero^{1,2},
7 Danny Incarnato⁴, Salvatore Oliviero^{2,5}, Laura Conti^{1,2}, Manuela Iezzi³, Daniela Tosoni⁶, Giovanni
8 Bertalot⁶, Stefano Freddi⁶, Francesco A. Tucci^{6,7}, Francesco De Santis⁸, Cristina Frusteri⁸, Stefano
9 Ugel⁸, Vincenzo Bronte⁸, Federica Cavallo^{1,2}, Paolo Provero⁹, Marta Gai¹, Daniela Taverna^{1,2}, Emilia
10 Turco¹, Salvatore Pece^{6,10*} and Paola Defilippi^{1,2**}.

11 ¹Department of Molecular Biotechnology and Health Sciences, University of Torino, Via Nizza 52,
12 10126, Torino, Italy.

13 ²Molecular Biotechnology Center (MBC) "Guido Tarone", Via Nizza, 52, 10126, Turin, Italy

14 ³Immuno-Oncology Laboratory, Center for Advanced Studies and Technologies; Department of
15 Neurosciences, Imaging and Clinical Sciences. G. d'Annunzio University of Chieti-Pescara, Italy

16 ⁴Department of Molecular Genetics, Groningen Biomolecular Sciences and Biotechnology Institute
17 (GBB), University of Groningen, Groningen, the Netherlands.

18 ⁵Department of Life Sciences and Systems Biology, University of Turin, Torino, Italy.

19 ⁶European Institute of Oncology IRCCS, 20141 Milan, Italy

20 ⁷School of Pathology, University of Milan, Milan, Italy.

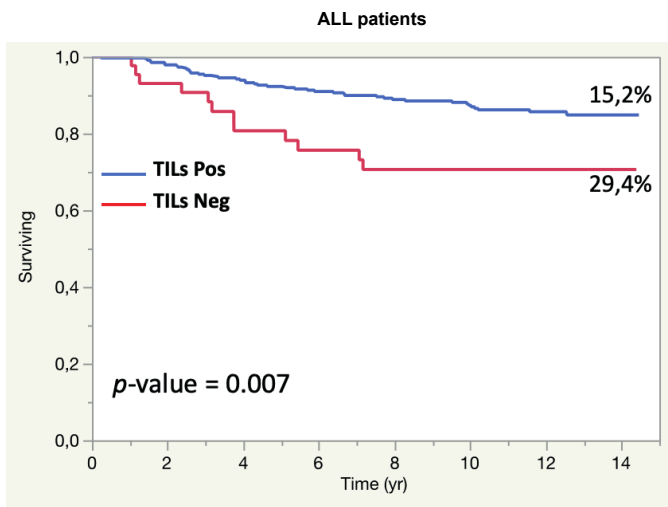
21 ⁸Immunology Section, Department of Medicine, University of Verona, 37134 Verona, Italy

22 ⁹Neuroscience Department "Rita Levi Montalcini", University of Torino, Via Cherasco 15, 10126
23 Torino, Italy.

24 ¹⁰Department of Oncology and Hemato-Oncology, Università degli Studi di Milano, 20142 Milano,
25 Italy.

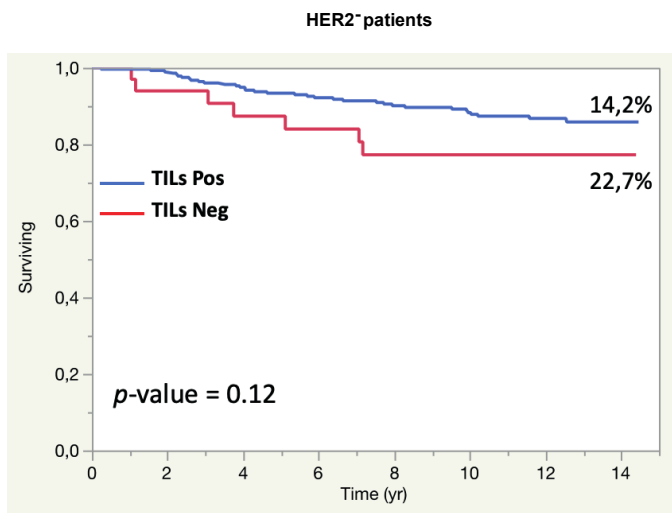
26 **Corresponding Author: Paola Defilippi (paola.defilippi@unito.it)

27 *Co-corresponding Author: Salvatore Pece (salvatore.pece@ieo.it)



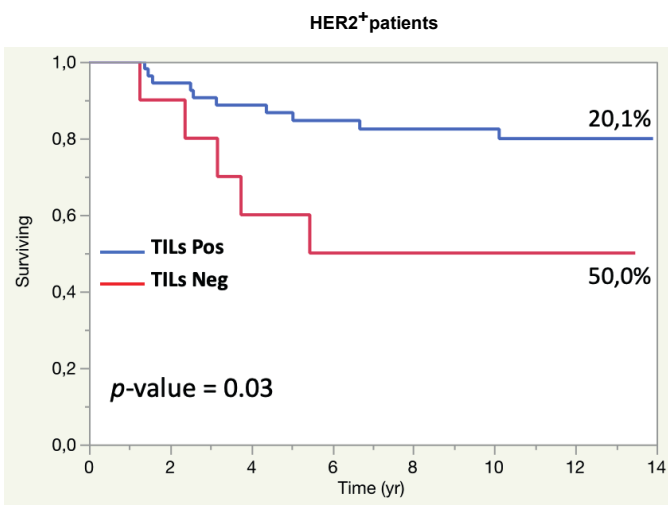
	TILs Neg	TILs Pos	Total
p140Cap Low	15 (36,5%)	66 (20,4%)	81
p140Cap High	26 (63,4%)	257 (79,5%)	283
Total	41	323	364

OR = 2,25 (1,13;4,48)
P = 0,02



	TILs Neg	TILs Pos	Total
p140Cap Low	11 (29,1%)	51 (19,0%)	62
p140Cap High	21 (65,6%)	217 (80,9%)	238
Total	32	268	300

OR = 2,23 (1,01;4,91)
P = 0,04



	TILs Neg	TILs Pos	Total
p140Cap Low	4 (44,4%)	15 (27,2%)	19
p140Cap High	5 (55,5%)	40 (72,7%)	45
Total	9	55	64

OR = 2,13 (0,50;9,03)
P = 0,30

30 **Supplementary Fig. 1**

31 Left, The overall survival rates of the negative and positive stromal TIL groups were analyzed using
32 Kaplan-Meier survival analysis, and the statistical significance of between-group differences was
33 evaluated using the Log-rank Test. Univariate and multivariate Cox regression analyses were
34 performed to identify the prognostic significance of stromal TILs. Right, Analysis of the distribution
35 of TIL-positive and TIL-negative female patients according to their p140Cap status (p140Cap^{HIGH} vs.
36 p140Cap^{LOW}) in all patients (top) and in the subgroup of HER2-negative (middle) and HER2-positive
37 (bottom) patients; p-value, Pearson's Chi-Squared Test.

38

39

40

41

42

43

44

45

46

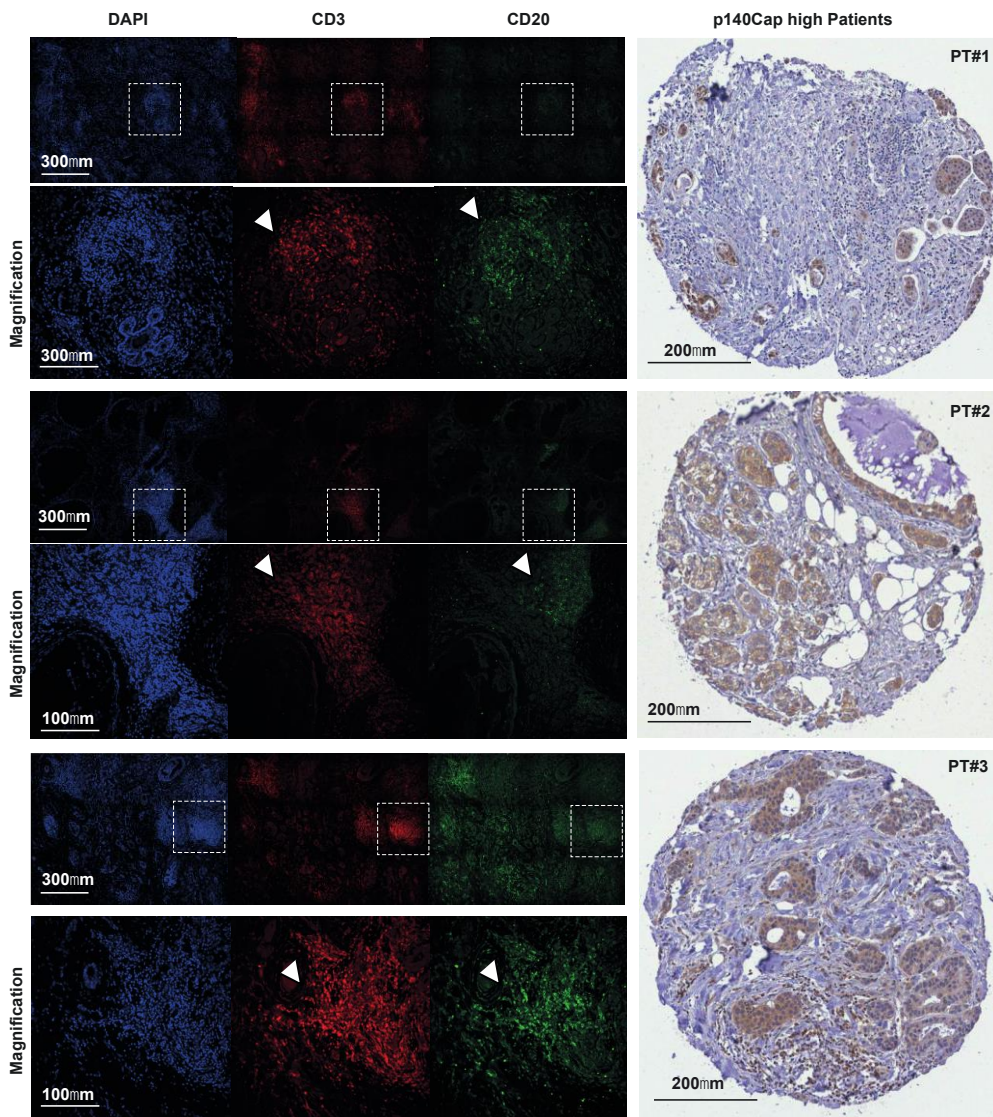
47

48

49

50

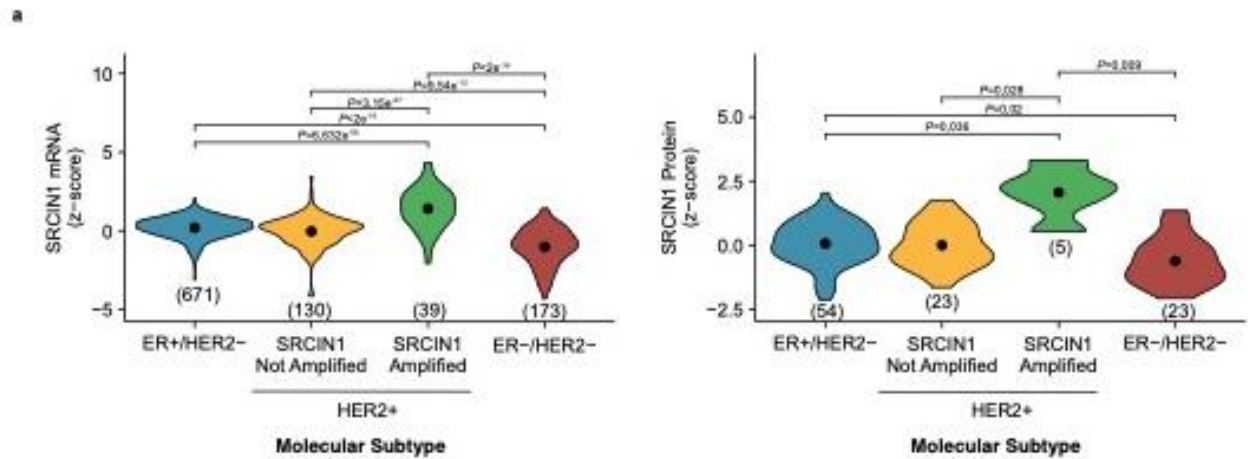
51



52

53 **Supplementary Fig. 2**

54 Left, Representative immunofluorescence images from the immunophenotypic characterization of
 55 the TIL infiltrate in n=3 different p140Cap^{HIGH} breast tumors performed on 3µm-thick FFPE sections
 56 using an anti-CD3 (red) and anti-CD20 (green) antibody to recognize T- and B-lymphocytes,
 57 respectively. For each tumor sample (n=3), a tile merge (top panels) of 12 representative regions of
 58 interest (ROI) acquired independently is shown for each staining (blu, DAPI; red, CD3; green, CD20).
 59 A representative ROI from the tile merge for each staining is magnified in bottom panels. Right,
 60 Representative immunohistochemistry images of the TMA cores of the three different p140Cap^{HIGH}
 61 breast tumors (PT#1-3). Scale bars are indicated.



b Correlation with p140Cap and molecular subtypes

	p140Cap High	p140Cap Low	Total	OR (CI)	p
ER+/HER2-	325 (80.7%)	78 (19.3%)	403	Reference	
HER2+	45 (67.2%)	22 (32.8%)	67	2.04 (1.16-3.59)	0.012
ER-/HER2-	16 (57.1%)	12 (42.9%)	28	3.13 (1.42-6.87)	0.0031
Total	386	112	498		

62

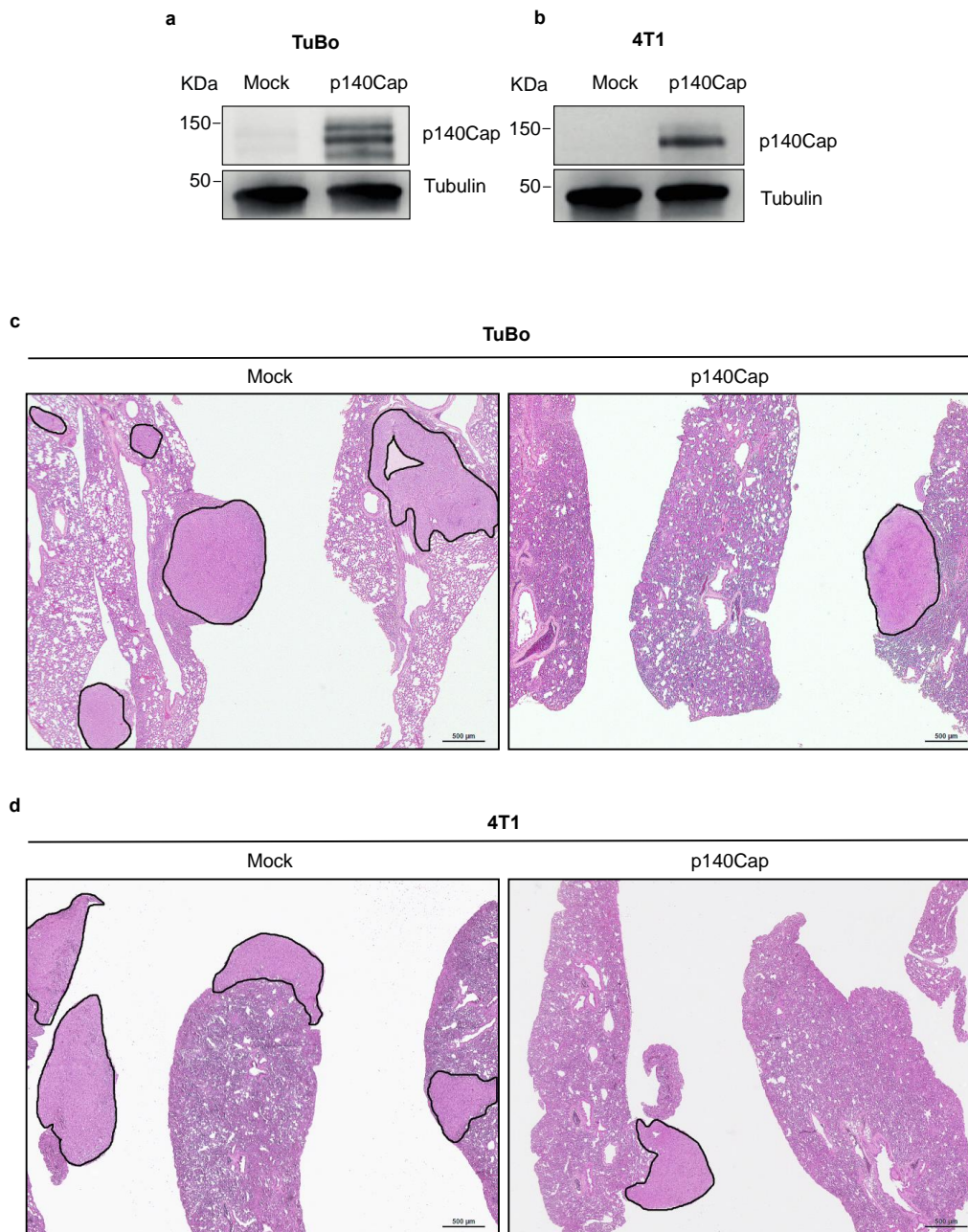
63

64

65 **Supplementary Fig. 3**

66 **a** Analysis of p140Cap expression across the different molecular subtypes of human BC. Violin plots
 67 show the expression levels of *SRCIN1* transcripts (left) and p140Cap protein (right) in different
 68 molecular subtypes of human BC patients from the 1095 BC female patients from TCGA-BRCA
 69 cohort³⁴. The black dots indicate the average. The number of patients for each subtype is shown in
 70 parentheses. For the HER2+ subtype, tumors with presence or absence of *SRCIN1* co-amplification
 71 are shown.

72 **b** Analysis of the distribution of p140Cap^{HIGH} and p140Cap^{LOW} female patients of the 498 BC female
 73 patients of the IEO cohort, see Methods, according to the different molecular subtypes: luminal
 74 (ER+/HER2-), HER2-amplified (HER2+) and triple-negative (ER-/HER2-); Odds Ratio (OR) with
 75 95% Confidence Intervals (CI) are indicated; p-value, Pearson's Chi-Squared Test.



77

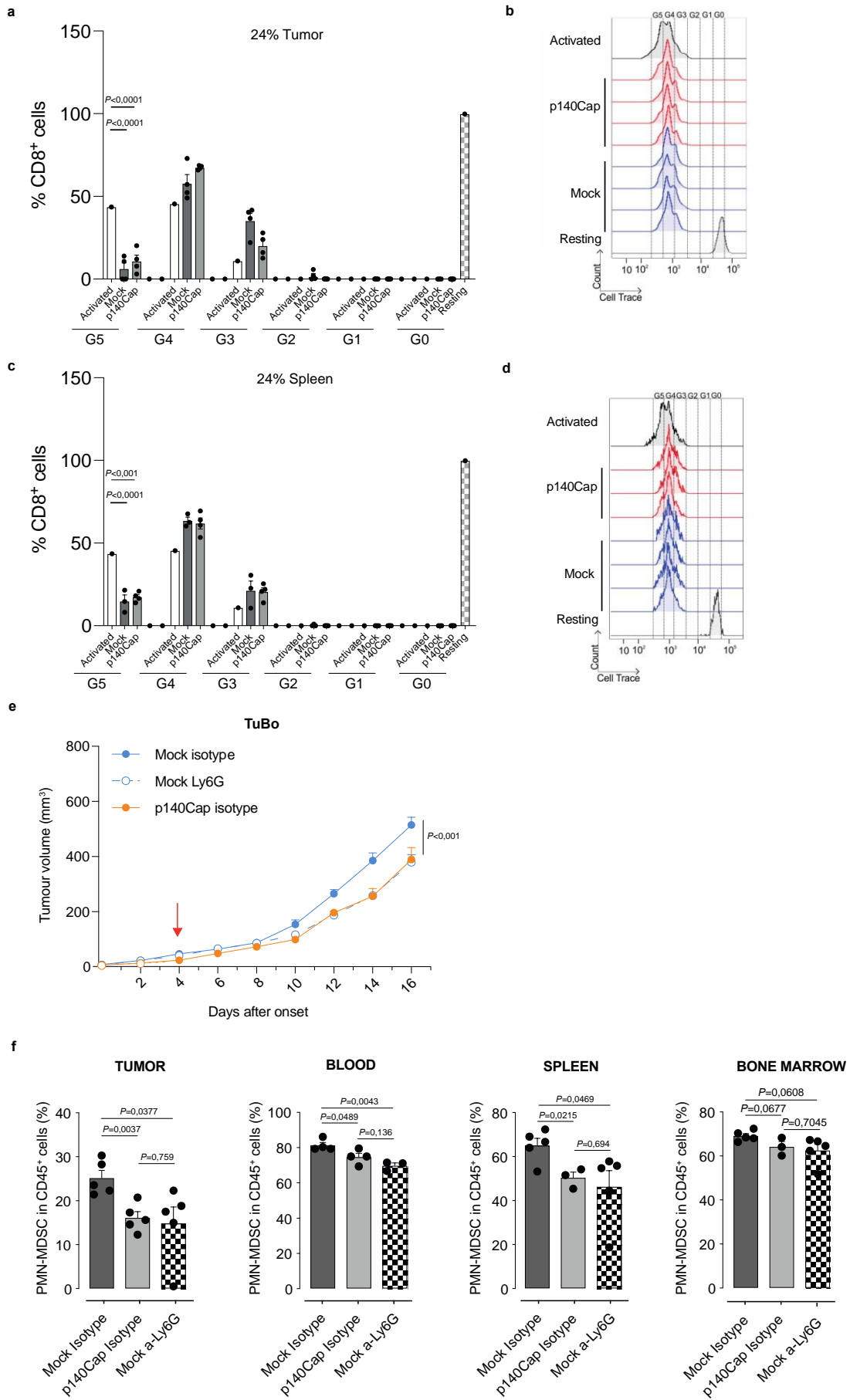
78 **Supplementary Fig. 4**

79 **a-b** Western Blot analysis of a pool of four clones with enforced p140Cap expression upon retroviral
 80 infection in TuBo in **a**, and 4T1 cells in **b** (n=10 experimental repeats). Tubulin was used as loading
 81 control.

82 **c-d** A set of representative H&E images of lung tissues from mice injected with mock or p140Cap
83 TuBo, or 4T1 cells, where each figure shows the metastatic area (see also Methods); TuBo, n=5 mice;
84 4T1, n= 10 mice.

85 .

86



88 **Supplementary Fig. 5**

89 Suppressive activity of tumor-infiltrating CD11b⁺ cells isolated from either p140Cap (red) or Mock
90 (blue) tumor-bearing mice co-cultured with activated T cells in presence, was evaluated by flow
91 cytometry tracking cell trace dilution in Cell Trace-labelled; peptide activated HA-specific T cells
92 after 3 days.

93 **a** Cell Trace dilution representative plots of CTLs co-cultured with 24% of tumor-isolated CD11b⁺
94 cells are shown. Data are represented for n=4 mice/group as mean \pm SEM; two-tailed unpaired *t* test.

95 **b** T cell proliferative generations (from G0 to G5) under resting condition (not activated by peptide,
96 grey line) or stimulated and co-cultured with CD11b⁺ cells derived from Mock-derived (blues) or
97 p14Cap (red) tumors. Data are represented for n=4 mice/group as mean \pm SEM; 2way ANOVA test.

98 G: generations. Suppressive activity of splenic Ly6G⁺ cells isolated from either p140Cap (red) or
99 Mock (blue) tumor-bearing mice co-cultured with activated T cells in presence was evaluated by flow
100 cytometry tracking cell trace dilution in Cell Trace-labelled; peptide activated HA-specific T cells
101 after 3 days.

102 **c** Cell trace dilution representative plots of CTLs co-cultured with 24% of splenic Ly6G⁺ cells. (D)
103 T cell proliferative generations (from G0 to G5) under resting condition (not activated by peptide,
104 grey line) or stimulated and co-cultured with Ly6G⁺ cells derived from Mock-derived (blues) or
105 p140Cap (red) tumors. Data are represented for n=4 mice/group as mean \pm SEM; 2way ANOVA test.

106 **e-f** In vivo anti-Ly6G treatment.

107 **e** 10⁵ TuBo Mock and p140Cap cells were injected into the mammary fat pad of female BALB/c
108 mice. When tumors size reached 80 mm³, anti-Ly6G antibody treatment was performed by two IP
109 injections per week, of 100 μ g of anti-Ly6G (n=5) or control IgG2a isotype antibodies (n=5/Mock
110 isotype; n=4/p140Cap isotype). Tumor growth was monitored and tumor size was measured. Data
111 are represented for n=5 mice/group as mean \pm SEM; 2way ANOVA test.

112 **f** Flow cytometry analysis for PMN-MDSCs. Representative flow cytometry bar plots showed the
113 percentage (%) of PMN-MDSC (CD45+CD11b+Ly6G+Ly6Clow) cells normalised on CD45+ cells,
114 in tumor (n=5), blood (n=4/Mock isotype; n=4/p140Cap isotype; n=3/Mock anti-Ly6G), spleen
115 (n=5/Mock isotype; n=3/p140Cap isotype; n=5/Mock anti-Ly6G) and bone marrow (n=5/Mock
116 isotype; n=3/p140Cap isotype; n=5/Mock anti-Ly6G) of mice treated as in (E) with anti-Ly6G and
117 anti-isotype administrations. Data are represented for n=x mice/group as mean \pm SEM; two-tailed
118 unpaired t test.

119

120

121

122

123

124

125

126

127

128

129

130

131

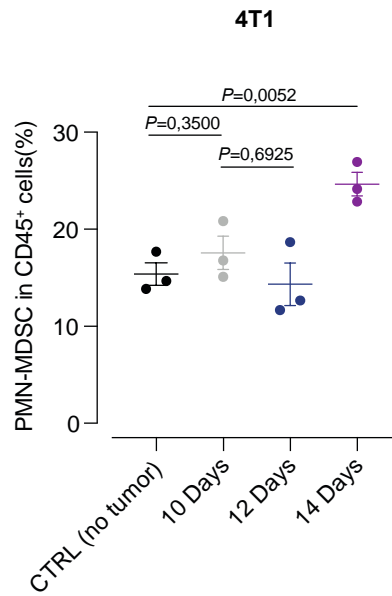
132

133

134

135

136



137

138

139 **Supplementary Fig. 6**

140 FACS analysis of PMN-MDSCs (CD45+CD11b+Ly6G+Ly6Clow) cells normalised on CD45+ cells
141 in lungs of Mock 4T1 tumor-bearing mice after 10, 12 and 14 days post-injection. Data are
142 represented for n=3 mice/group; dot plot represented as mean \pm SEM; two-tailed unpaired t test.

143

144

145

146

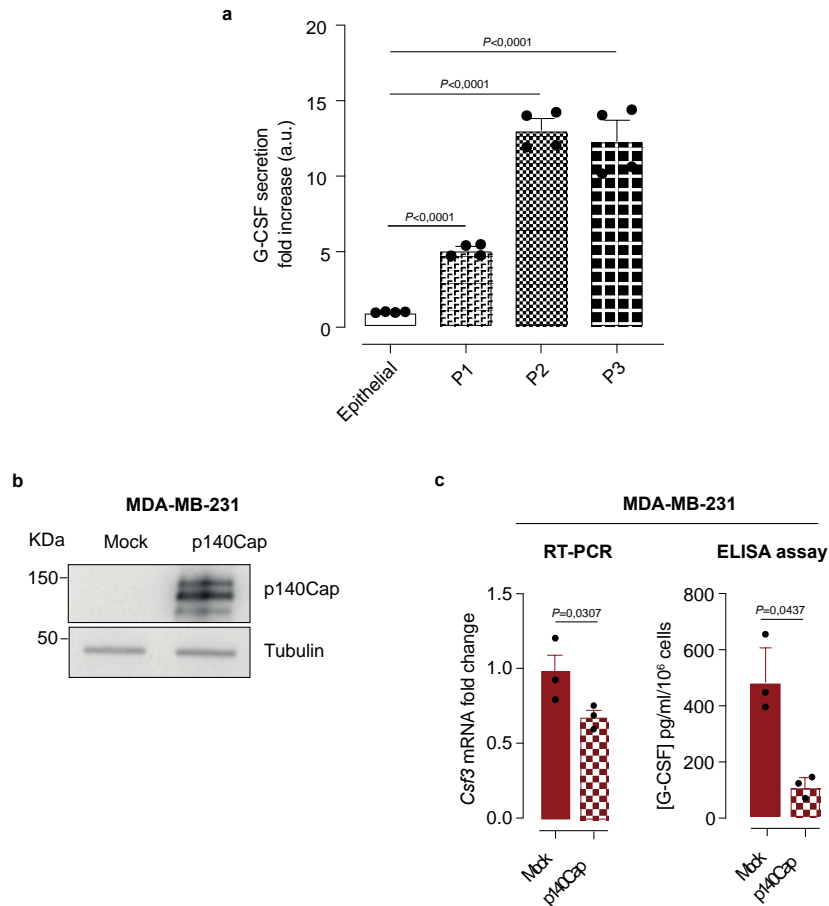
147

148

149

150

151



152

153

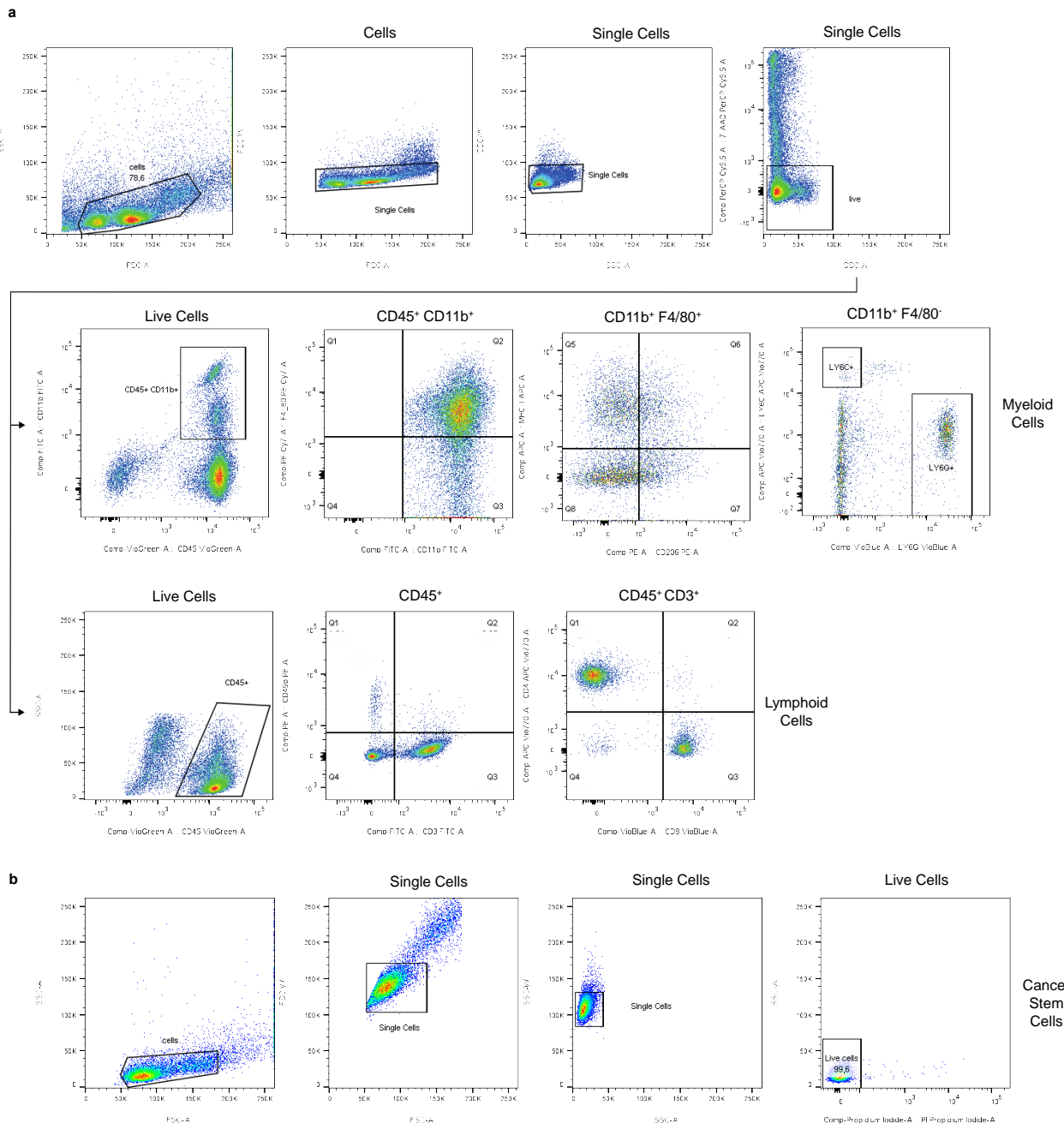
154 **Supplementary Fig. 7**

155 **a** ELISA assay of G-CSF secretion in Mock TUBO cell culture supernatants and in P1, P2 and P3
156 mammosphere supernatants. Data are represented for n=4 experimental repeats; bar plot represented
157 G-CSF fold increase as mean \pm SEM; two-tailed unpaired t test.

158 **b** Generation of MDA-MB-231 p140Cap overexpressing cells. Western Blot analysis of a pool of
159 four clones of MDA-MB-231 cells expressing p140Cap upon retroviral infection. Data are
160 represented for n=10 experimental repeats. Tubulin was used as loading control.

161 c G-CSF transcript and G-CSF protein levels were measured in Mock and p140Cap MDA-MB-231
162 cells, by quantitative RT-PCR or by ELISA on cell culture supernatants, respectively. Data are
163 represented for n=3 experimental repeats, bar plot represented as mean \pm SEM; two-tailed unpaired t
164 test.

165



167

168

169 **Supplementary Fig. 8**

170 **a** Gating strategy for the tumor immune infiltrate in Figure 2 (panel **b-d**), Figure 4 (panel **a-b**), Figure
 171 6 (panel **j**), Figure 9 (panel **f**)

172 **b** Gating strategy for the Cancer Stem Cell markers in Figure 5 (panel **d-e**).